Science of the Total Environment 698 (2020) 133860

Contents lists available at ScienceDirect

Science of the Total Environment

journal homepage: www.elsevier.com/locate/scitotenv

Long-term exposure to 4G smartphone radiofrequency electromagnetic radiation diminished male reproductive potential by directly disrupting Spock3–MMP2-BTB axis in the testes of adult rats

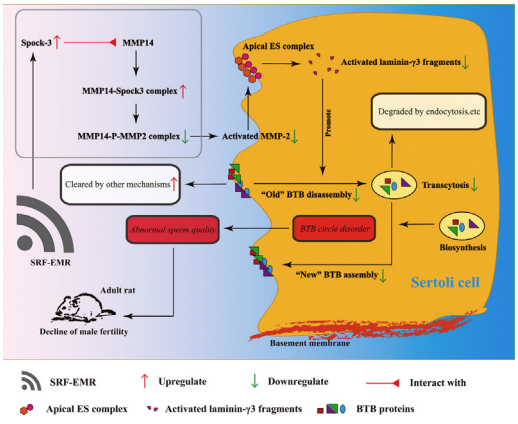
Gang Yu [a,b,1], Zeping Tang [c], Hui Chen [d], Zhiyuan Chen [d], Lei Wang [d], Hui Cao [e], Gang Wang [a], Jiansheng Xing [a], Haotao Shen [f], Qing Cheng [a], Donghui Li [a], Guoren Wang [a], Yang Xiang [a], Yupeng Guan [a,b], Yabing Zhu [g], Zhenxiang Liu [a], Zhiming Bai [a,b,*]

[a] Department of Urology, Affiliated Haikou Hospital of Xiangya School of Medicine, Central South University, Haikou, Hainan Province, China
[b] Haikou Center for Medical Synchrotron Radiation Research, Haikou People's Hospital, Haikou, Hainan Province, China
[c] Guangdong Environmental Radiation Monitoring Center, Guangzhou, Guangdong Province, China
[d] Hubei Key Laboratory of Urology, Renmin Hospital of Wuhan University, Wuhan, Hubei Province, China
[e] Central Laboratory of Affiliated Haikou Hospital of Xiangya School of Medicine, Central South University, Haikou, Hainan Province, China
[f] Shenzhen Academy of Information and Communications Technology, Shenzhen, Guangdong Province, China
[g] Department of Critical Care Medicine, Renmin Hospital of Wuhan University, Wuhan, Hubei Province, China

HIGHLIGHTS

- Long-term exposure to smartphone RF-EMR suppressed male fertility.
- Smartphone RF-EMR exposure directly impaired testes and upregulates testicular Spock3.
- Inhibiting Spock3 overexpression restored sperm quality and alleviated testicular injury.
- Smartphone RF-EMR directly impaired testes by regulating Spock3–MMP2–BTB axis.

GRAPHICAL ABSTRACT



ARTICLE INFO

Article history:
Received 6 May 2019
Received in revised form 6 August 2019
Accepted 8 August 2019
Available online 31 August 2019

ABSTRACT

The correlation between long-term exposure to SRF-EMR and the decline in male fertility is gradually receiving increasing attention from the medical society. While male reproductive organs are often exposed to SRF-EMR, little is currently known about the direct effects of long-term SRF-EMR exposure on the testes and its involvement in the suppression of male reproductive potential. The present study was designed to investigate this issue by using 4G SRF-EMR in rats. A unique exposure model using a 4G smartphone achieved localized exposure to

Abbreviations: SRF-EMR, smartphone radiofrequency electromagnetic radiation; 4G, the 4th generation mobile communication technology; Spock3, SPARC/osteonectin, cwcv and kazal like domains proteoglycan 3; BTB, blood-testis barrier; MMP2, matrix metallopeptidase 2; MMP14, matrix metallopeptidase 14.

* Corresponding author at: Department of Urology, Affiliated Haikou Hospital of Xiangya School of Medicine, Central South University, Haikou, Hainan Province, China.
E-mail address: Drzmbai@163.com (Z. Bai).

[1] The first author: Dr.

https://doi.org/10.1016/j.scitotenv.2019.133860
0048-9697/© 2019 Elsevier B.V. All rights reserved.

Editor: Wei Huang

Keywords:
Smartphone radiofrequency electromagnetic radiation
4th generation mobile communication technology
Male reproductive potential
Testis
SPARC/osteonectin, cwcv and kazal like domains proteoglycan 3
Blood-testis barrier

the scrotum of the rats for 6 h each day (the smartphone was kept on active talk mode and received an external call for 1 min over 10 min intervals). Results showed that SRF-EMR exposure for 150 days decreased sperm quality and pup weight, accompanied by testicular injury. However, these adverse effects were not evident in rats exposed to SRF-EMR for 50 days or 100 days. Sequencing analysis and western blotting suggested Spock3 overexpression in the testes of rats exposed to SRF-EMR for 150 days. Inhibition of Spock3 overexpression improved sperm quality decline and alleviated testicular injury and BTB disorder in the exposed rats. Additionally, SRF-EMR exposure suppressed MMP2 activity, while increasing the activity of the MMP14–Spock3 complexes and decreasing MMP14–MMP2 complexes; these results were reversed by Spock3 inhibition. Thus, long-term exposure to 4G SRF-EMR diminished male fertility by directly disrupting the Spock3–MMP2–BTB axis in the testes of adult rats. To our knowledge, this is the first study to show direct toxicity of SRF-EMR on the testes emerging after long-term exposure.

© 2019 Elsevier B.V. All rights reserved.

1. Introduction

Smartphones, when in use, emit a type of non-ionizing radiation called smartphone radiofrequency electromagnetic radiation (SRF-EMR) (IARC, 2013). The standard frequency of SRF-EMR emitted by smartphone is primarily in the range of 500–3000 Mhz. SRF-EMR is considered to be different from other types of radiofrequency electromagnetic radiation as it primarily affects surrounding objects through unclear non-thermal effects instead of thermal effects (Agarwal et al., 2011; Bolte and Eikelboom, 2012). With the widespread use of smartphones, the concern for health problems caused by SRF-EMR has gradually become a worldwide subject of interest (Belpomme et al., 2018; Eeftens et al., 2018; Viel et al., 2009).

At present, SRF-EMR is believed to cause some specific neurological disorders and even increase the risks of certain cancers, which have been widely discussed in the medical society (Bielsa-Fernandez and Rodriguez-Martin, 2018; Falcioni et al., 2018; Kwon and Hamalainen, 2011; Repacholi et al., 2012; Vahedi and Saiphoo, 2018). However, its biological effects—especially its long-term effects—on male fertility have remained ambiguous and relatively rarely investigated, only recently drawing the attention of the medical society (Houston et al., 2016; Kesari et al., 2018; Liu et al., 2014; Santini et al., 2018; Sepehrimanesh and Davis, 2016). Most relevant studies have primarily focused on SRF-EMR exposure on the whole body or head region while few have explored its direct biological effects on the testis, which could further reveal the specific biological effect of SRF-EMR on male fertility (Adams et al., 2014). As most men prefer to carry smartphones in their trouser pockets, close to the testes, some scholars speculate whether this habit aggravates the subfertility of contemporary men (Sepehrimanesh et al., 2017; Yan et al., 2007). Thus, clarifying whether SRF-EMR could exert any direct biological effect on the testes could help us to better address this confusion, and help avoid potential adverse reproductive effects of SRF-EMR.

Thus, the present study established a special 4G (4G: the 4th generation mobile communication technology) SRF-EMR exposure model with a smartphone in rats and aimed to investigate whether this currently-used SRF-EMR in daily communication could affect male reproductive potential by directly affecting the testes.

2. Materials and methods

2.1. Animals, antibodies and grouping

All of the male adult Sprague-Dawley rats (12 weeks) underwent 7 days of housing acclimation before the experiment. All the experimental procedures were approved by the Experimental Animal Care and Use Committee in the Affiliated Haikou Hospital of Xiangya School of Medicine and all the experimental procedures were performed in accordance with international animal care guidelines. The primary antibodies used in this study are listed in Table S1.

To investigate the reproductive effect of SRF-EMR, a total of 135 rats were randomly distributed at three time points (50 days, 100 days and 150 days) for further analysis. At each time point, the rats were randomly divided further into three groups: Nor group ($n = 15$), rats living in the cages without any intervention; Con group ($n = 15$), rats kept in the customized units without exposure to SRF-EMR; and SRF group ($n = 15$), rats kept in the customized units and exposed to SRF-EMR.

To investigate the mechanisms leading to SRF-EMR reproductive toxicity, rats were randomly divided into seven groups: Nor group ($n = 10$), rats living in the cages without any intervention; Con group ($n = 10$), rats kept in the units without exposure to SRF-EMR and injected with normal saline (intratesticular injection); LV-SP3 group ($n = 13$), rats kept in the units without exposure to SRF-EMR and injected with LV-Spock3 (Spock3: SPARC/osteonectin, cwcv and kazal like domains proteoglycan 3) lentivirus (intratesticular injection); LV-NC group ($n = 13$), rats kept in the units without exposure to SRF-EMR and injected with LV-NC lentivirus (intratesticular injection); SRF group ($n = 15$), rats kept in the units, exposed to SRF-EMR and injected with normal saline (intratesticular injection); SRF + LV-SP3 group ($n = 15$), rats kept in the units, exposed to SRF-EMR and injected with LV-Spock3 lentivirus (intratesticular injection); and SRF + LV-NC group ($n = 15$), rats kept in the units, exposed to SRF-EMR and injected with LV-NC lentivirus (intratesticular injection).

2.2. SRF-EMR exposure system and experimental setup

As shown in Fig. 1A and Fig. 1B, a customized unit full of air holes was made and a 4G smartphone emitting SRF-EMR was placed under the unit. To achieve local exposure, electromagnetic-blocking material was attached to the bottom of each unit with an opening left to allow the testes of rats to be exposed to SRF-EMR. Each unit had a slope at the bottom that allowed the testes to descend into the scrotum naturally when the rats relaxed. Pieces of rough cloth were fixed to the floor of each unit in order to improve the animals' footing and maintain the exclusive smell of each rat.

As Fig. 1C shows, during the experimental treatment, the rats of the Con group or the SRF group stayed in the customized units with smartphones. The smartphones were working to produce SRF-EMR in the SRF group while the phones were off to achieve sham-exposure in the Con group. There were electromagnetic-blocking walls between the adjacent exposure units to reduce the interaction of SRF-EMR from each unit. To construct optimal experimental conditions, the experiment was conducted in a quiet room with controlled temperature and ventilation.

Before the official experiment, rats were acclimated to the units for one week. All the rats were kept in their exclusive units to nullify mental stress in the experiment. To further confirm mental stress was eliminated in these confined rats, serum cortisol levels were evaluated after

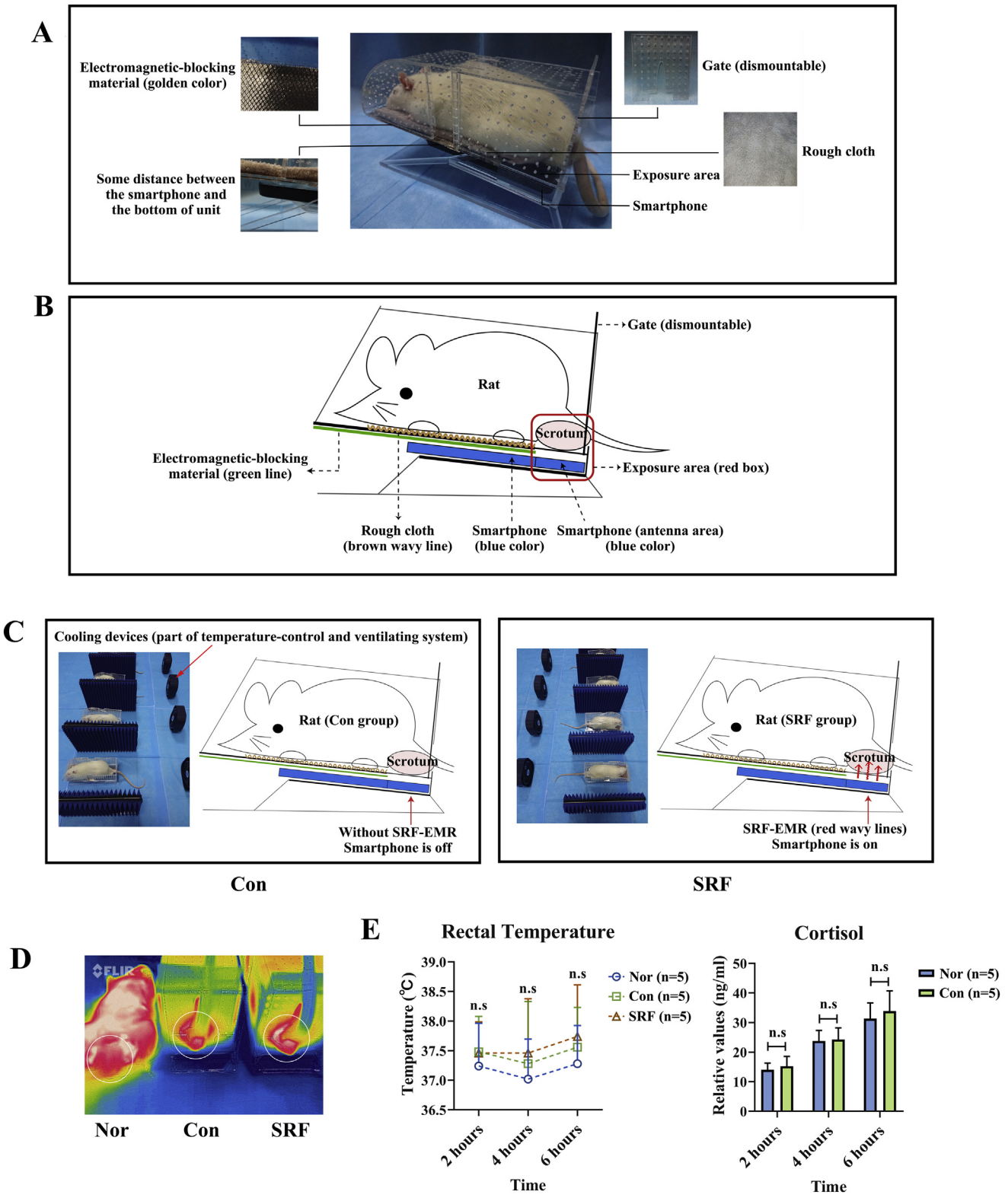


Fig. 1. SRF-EMR exposure system in the experiment. A customized unit was made to ensure local exposure (testicular area) in a temperature-controlled room. All the rats were kept in their exclusive units during the experiment. To determine whether this unit leads to hyperthermia and mental stress in rats, scrotal temperature, rectal temperature, and serum cortisol were recorded during the 6 h experiment duration. The experimental treatment did not significantly increase body temperature and serum cortisol in rats. (A) Representative image and (B) schematic diagram of the customized unit. Numerous air holes were created to ensure efficient air circulation. Each unit had a slope at the bottom which that allowed the testes to naturally descend into the scrotum, to ensure exposure to the SRF-EMR. Localized SRF-EMR exposure was achieved by attaching electromagnetic-blocking material to the bottom of the entire unit except for the exposed scrotum area. (C) Representative images and schematic diagrams showing how the rats were sham-exposed in the Con group or exposed in the SRF group during the experiment. The cooling devices in the images were used to further control the scrotum temperature. (D) Representative thermography image of rats ($n = 5$); the scrotal area has been included in the white round frame. After 6 h of exposure, thermography did not show any significant difference in the scrotum temperature among the three experiment groups. (E) Values of rectal temperature and serum cortisol in rats. No significant differences are observed in the rectal temperature and serum cortisol among the three experiment groups during the experimental treatment. Each value in histogram represents Mean ± SD. Abbreviation, n.s: no significant difference ($P > 0.05$).

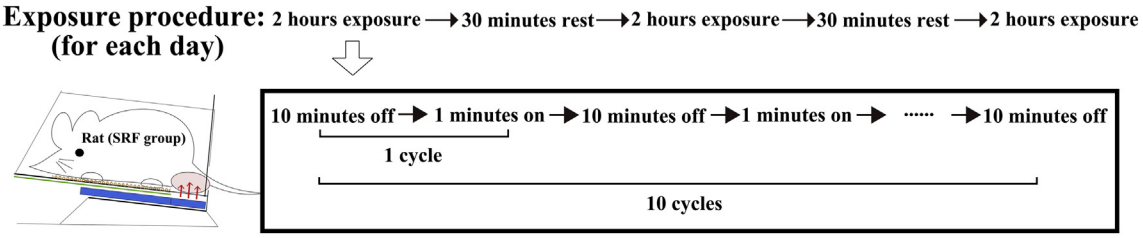


Fig. 2. Flow chart showing SRF-EMR exposure procedure. The smartphone under the scrotum of a rat was kept in talk mode for 6 h/day and received an external call that was held for 1 min with 10 min intervals. During the experimental treatment, the rats were released to have a rest for 30 min every 2 h. During the "10 minutes off" time frame, the phone was kept in talk mode. During the "1 minute on" timeframe, an external call was allowed to ring for 1 min with the phone concurrently remaining in talk mode.

the adaptation period. In addition, scrotal and rectal temperatures were monitored to observe any temperature change in these rats.

The official experiment was performed as follows: During the experimental treatment, rats were housed in the units. As the flow chart (Fig. 2) shows, the smartphone under the scrotum of a rat was kept in talk mode for 6 h/day and received an external call that was held for 1 min with 10 min intervals for consecutive 150 days. During the experimental treatment, the rats were released to have a rest for 30 min every 2 h. The smartphones were kept in silent mode to maintain a calm environment for the rats.

2.3. Construction and transfection of lentivirus

Three different siRNA duplexes (Table S2) targeting Spock3 and scrambled siRNA duplex were synthesized by GenePharma Co., Ltd (Shanghai, China), and a screening test was performed with the C6 rat glioma cell line (provided by the Cell Bank of Central South University) to select the most efficient one. The sequence of the chosen siRNA duplex was then used to construct a lentivirus transfection system by GenePharma. In this system, the pGag/Pol, pRev, pVSV-G packaging plasmid and LV3(H1/GFP&Puro) shuttle plasmid were used. The Rat Spock3 shRNA sequence of LV-Spock3 lentivirus was 5'-GCTCACACA CAGTATGAAA-3′ and the scrambled shRNA sequence of LV-NC lentivirus was 5′-TTCTCCGAACGTGTCACGT-3′. The final virus titer was 5×10^9 TU/ml.

Rats exposed to SRF-EMR for 100 days were transfected with LV-Spock3 lentivirus via intratesticular injection to knock down Spock3 in their testes as described in previous studies (Wu et al., 2012; Zohni et al., 2012). The successful transfection was detected by bioluminescence imaging and western blotting.

2.4. RNA-sequencing and bioinformatics

For this particular study, rats with sperm concentration close to average values were selected from both Con and SRF groups, and mRNA-sequencing was performed as follows. Total RNA was extracted and sequencing was performed with BGISEQ-500 platform (BGI Genomics Institute, Wuhan, China). The total RNA sample quality check was analyzed with Agilent 2100 Bioanalyzer and SOAPnuke was used to filter reads and obtain clean reads for further analysis. Differentially expressed genes (DEGs) were detected using DEGseq as described by Wang (Wang et al., 2010).

2.5. Statistical analysis

All statistical analyses were performed using SPSS 23.0. The quantitative data meeting normal distribution were presented as mean ± standard deviation (SD), while those meeting non-normal distribution were presented as median (interquartile range). Student's *t*-test or Mann–Whitney *U* test was performed for the statistical comparison of two groups, while one-way analysis of variance (ANOVA), two-way ANOVA, or Kruskal–Wallis H test was performed for the comparison of three or more groups. For the post-hoc test of ANOVA, Bonferroni test was used for data with homogeneous variance, whereas Games-Howell test was used for data with heterogeneous variance. The counting data in the mating experiment were compared using Fisher exact test. Pearson correlation analysis was used to evaluate the correlation of results. $P < 0.05$ was considered as statistically significant.

2.6. General methods

Other methods including dosimetry analysis, sperm quality analysis, mating experiment, bioluminescence imaging, histopathology, western blotting, and co-immunoprecipitation can be found in *Supplementary materials and methods.*

3. Results

3.1. Experimental treatment did not significantly increase body temperature and serum cortisol levels in rats

The frequency band of the smartphones was 2575–2635 MHz (TD-LTE). The electric field strength, power density of SRF-EMR, and SAR in the exposure area were respectively 37.93 V/m, 22.74 W/m^2 and 1.05 W/kg. As shown in Fig. 1D–E, the smartphone did not significantly increase the scrotal temperature or the rectal temperature of the rats during the experimental treatment. No significant increase in the serum cortisol levels was observed in the rats of the Con group compared with the Nor group. These results indicated that the experimental treatment did not cause significant the abnormal scrotal temperature and mental stress, which is crucial to study the non-thermal effects of SRF-EMR on the testes of rats.

3.2. Long-term exposure to SRF-EMR diminished male fertility potential

As shown in Fig. 3A, after 50 days of SRF-EMR exposure, no significant differences in sperm quality were observed among the different groups. Furthermore, compared to the Con group, the group exposed to SRF-EMR for 100 days showed a slight decrease in sperm motility and sperm viability. However, no statistical significance was observed in sperm concentration and morphology between the two groups. After 150 days of SRF-EMR exposure, sperm concentration, motility, viability, and normal morphology were comparatively lower in the SRF group than in the Con group. During the whole experiment, no significant differences were observed in sperm quality between the Nor and Con groups. These results suggested that long-term SRF-EMR exposure could suppress sperm quality in rats.

The mating experiment was conducted to further evaluate the male fertility potential in rats exposed to SRF-EMR for 150 days. As shown in Fig. 3B, the pup weight was comparatively lower in the

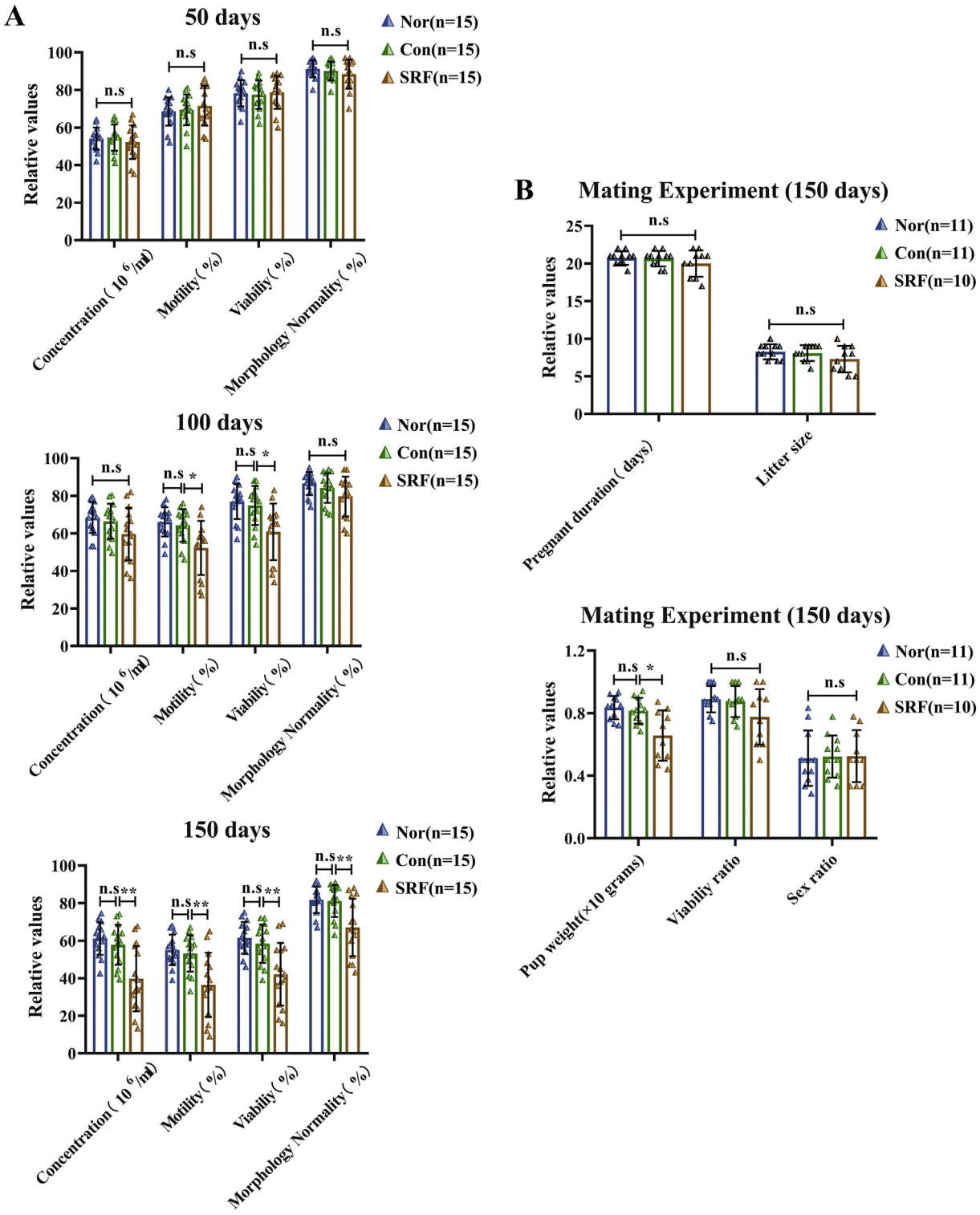


Fig. 3. Long-term exposure to SRF-EMR diminished male fertility potential. Male fertility potential was evaluated via sperm quality and mating experiment. (A) Relative values of sperm quality of rats in the experiment. SRF-EMR did not significantly impair sperm quality until 150 days after exposure. (B) Data from the mating experiment in the male rats exposed to SRF-EMR for 150 days. SRF-EMR significantly decreased the successful mating rate and pup weight of these rats. Each bar in histogram represents Mean ± SD. Abbreviation and symbol, n.s: no significant difference ($P > 0.05$), *: $P < 0.05$, **: $P < 0.01$.

SRF group than in the Con group, whereas no significant difference was observed in the successful mating percentage (Table 1), pregnancy duration, litter size, viability ratio or sex ratio between these two groups (Fig. 3B). Additionally, no significant differences in these indexes were found between the Nor and Con groups (Fig. 3B).

Table 1
Percentage of successful mating rats (male).

	Successful mating rats	Unsuccessful mating rats	Percentage	*P* value
Nor group	12	3	80.0%	0.587
Con group	13	2	86.7%	
SRF group	10	4	71.4%	

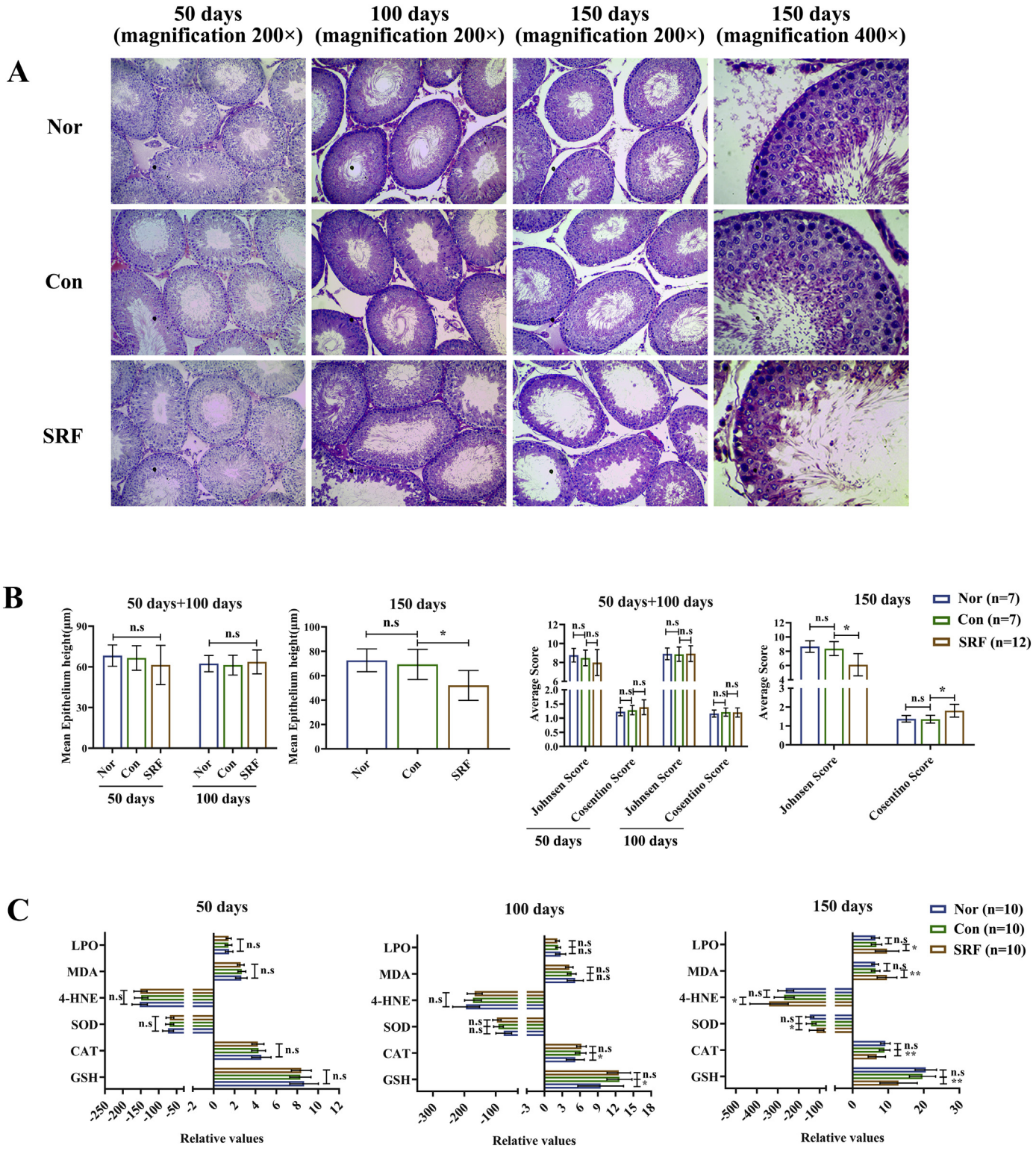


Fig. 4. Long-term SRF-EMR exposure directly impaired the testes of rats. The testicular injury was evaluated by analyzing H&E staining, the oxidation–antioxidation system and apoptosis in rats. (A-B) Representative images and morphologic scores of H&E staining in rat testes (original magnification 200× or 400×). Spermatogenesis disorder and seminiferous epithelium injury could be found in rats exposed to SRF-EMR for 150 days. Further analysis showed that SRF-EMR did not significantly decrease the epithelium height and Johnsen score, while increasing the Cosentino score in rats after 150 days of exposure. (C) Relative values of oxidative stress products and antioxidative enzymes in the testes of rats. SRF-EMR significantly upregulated LPO, MDA and 4-HNE and downregulated SOD, CAT and GSH after 150 days of exposure, but it only significantly downregulated CAT and GSH after 100 days of exposure in rats. (D–E) Representative western-blotting images and relative density changes of apoptosis proteins in the testes of rats. SRF-EMR did not lead to significant testicular apoptosis in rats until after 150 days of exposure. Each bar in histogram represents Mean ± SD. Abbreviation and symbol, P-Caspase: precursor caspase, C-Caspase: cleaved caspase, n.s: no significant difference ($P > 0.05$), *: $P < 0.05$, **: $P < 0.01$.

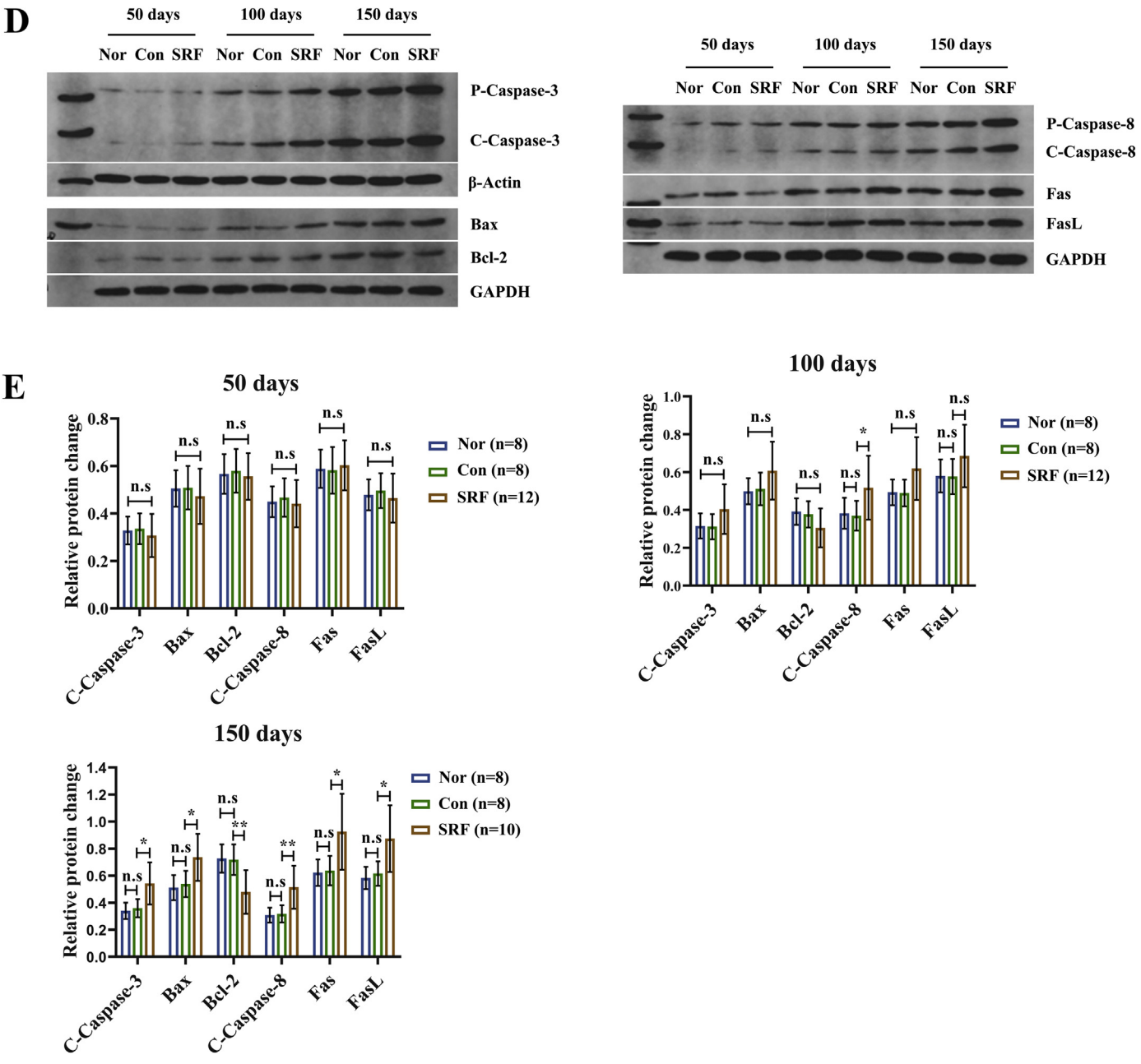


Fig. 4 (*continued*).

3.3. Long-term SRF-EMR exposure directly impaired testes

As shown in Fig. 4A–B, after 50 days of experiment, hematoxylin and eosin staining showed normal testicular architecture and orderly spermatogenesis in rats of all three experiment groups. Additionally, no significant differences were observed in the mean epithelium height, or Johnsen score and Cosentino score among these three groups. After 100 days of experiment, although less orderly spermatogenesis and decreased epithelium height could be occasionally observed in rats of the SRF group, no statistically significant differences were observed in the mean epithelium height, Johnsen score or Cosentino score among the three experiment groups. After 150 days of experiment, increased disorder in spermatogenesis, as well as significant germ cell loss, and decreased epithelium height were observed in the SRF group. Lower epithelium height, lower Johnsen score, and higher Cosentino score was also observed in the SRF group when compared with the Con group, while no significant differences were noted between the Nor and Con groups. These results suggested that long-term SRF-EMR exposure directly led to testicular morphologic injury in rats.

The oxidation–antioxidation system was evaluated in the testes of rats. As shown in Fig. 4C, no significant differences were found among all three experiment groups after 50 days of SRF-EMR exposure. After 100 days of exposure, only CAT and GSH content was found to be significantly lower in the SRF group than in the Con group. After 150 days of exposure, the levels of MDA, 4-HNE and LPO were comparatively higher while GSH, SOD and CAT content were lower in the SRF group compared with the Con group. Together, these results indicated that long-term exposure to SRF-EMR increased oxidative stress in the testes of rats.

Testicular apoptosis was further investigated in this study. As shown in Fig. 4D–E, for the rats exposed to SRF-EMR for 50 days, no significant

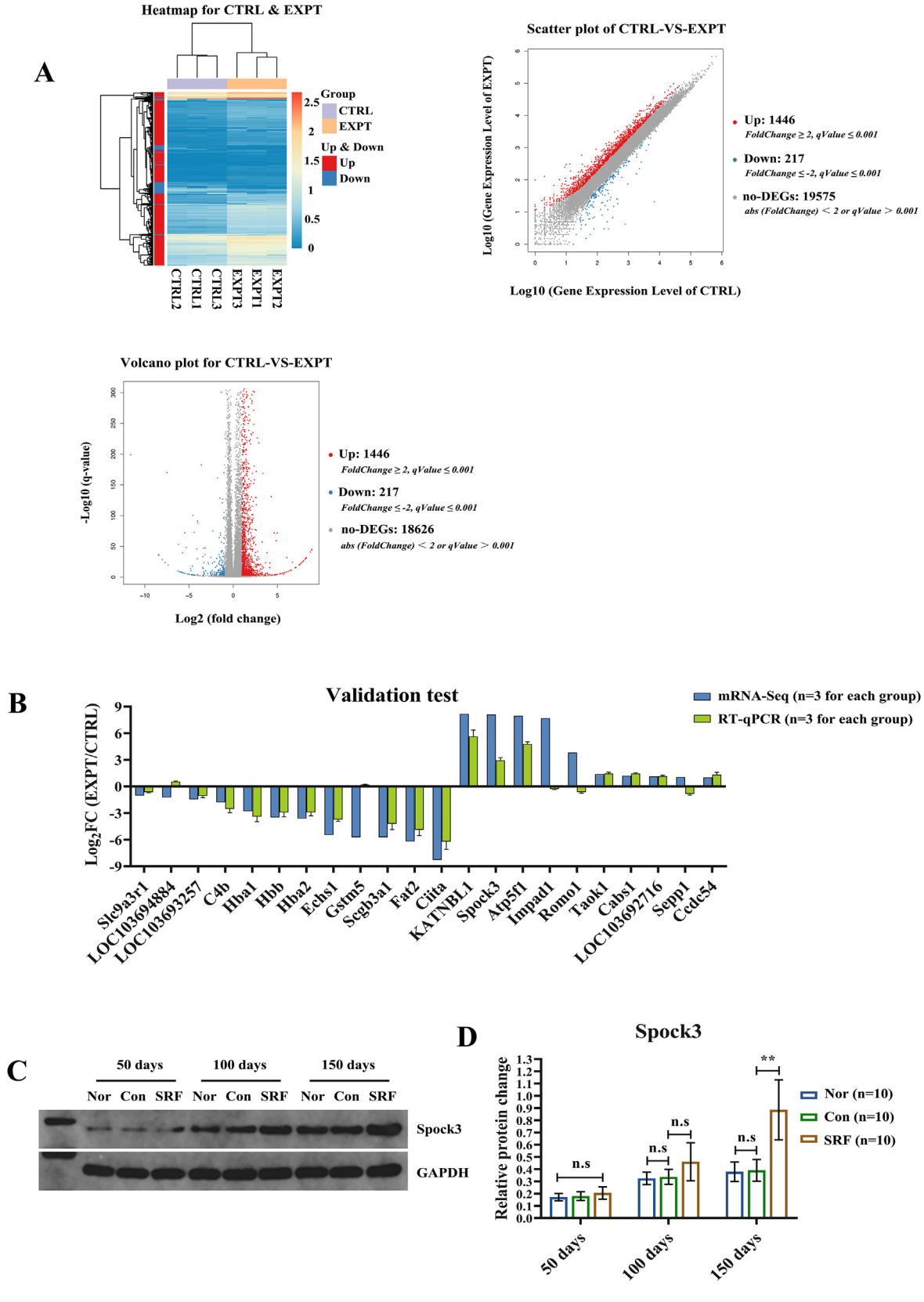


Fig. 5. SRF-EMR exposure upregulates testicular Spock3. Further changes in the testes were analyzed via mRNA-sequencing, RT-qPCR and western blotting in rats exposed to SRF-EMR for 150 days. CTRL group represents the Con group while EXPT group represents the SRF group. (A) Heatmap, scatter plot and volcano plot of mRNA-sequencing results($n = 3$). A total of 1663 differentially expressed genes (1446 up-regulated and 217 down-regulated genes) were identified. (B) Validation test for evaluating the accuracy of mRNA-seq. Genes with log2 fold change higher than 1 and p-value <0.002 in mRNA-seq were selected for validation. Log_2 fold change comparison and Pearson correlation analysis between mRNA-seq and RT-qPCR results were conducted in different groups. For 77.27% selected genes, concordant change patterns could be observed between mRNA-seq and RT-qPCR results. And there was a positive correlation ($R = 0.843$, $P < 0.001$) between mRNA-Seq and RT-qPCR results. (C–D) Representative western-blotting images and relative density changes of Spock3 in the testes of rats. The protein level of Spock3 in rats was not significantly upregulated until 150 days after exposure to SRF-EMR. Each bar in histogram represents Mean ± SD. Abbreviation and symbol, Log_2FC: Log_2 (fold change), n.s: no significant difference ($P > 0.05$), *: $P < 0.05$, **: $P < 0.01$.

Table 2
Differentially expressed genes with log2 Ratio(EXPT/CTRL) higher than 8 and q-value <0.01 in mRNA-seq.

Gene ID	Log2Ratio (EXPT/CTRL)	Regulation (EXPT/CTRL)	Q-Value	Symbol	Full Name
BGI_novel_G000649	8.889194	Up	1.33E-45	NA	NA
100911672	8.862017	Up	6.29E-45	LOC100911672	Atrophin-1 isoform X2
306079	8.731514	Up	8.36E-42	LOC306079	Ribosomal protein L14
100363502	8.728118	Up	1.00E-41	LOC100363502	Cytochrome c, somatic-like
BGI_novel_G000425	8.277055	Up	1.74E-32	NA	NA
312480	8.237696	Up	8.85E-32	Pcgf1	Polycomb group RING finger protein 1
691543	8.18087	Up	8.71E-31	Katnbl1	KATNB1-like protein 1
306404	8.113169	Up	1.21E-29	Spock3	SPARC/osteonectin, cwcv and kazal like domains proteoglycan 3
BGI_novel_G000359	−8.0216	Down	3.03E-29	NA	Serine/threonine-protein phosphatase 2A 55 kDa regulatory subunit B delta isoform isoform X1
85483	−8.28302	Down	0	Ciita	Class II, major histocompatibility complex, transactivator
BGI_novel_G000711	−8.40931	Down	2.48E-36	NA	NA
100911229	−8.45679	Down	2.65E-37	LOC100911229	Sperm motility kinase-like, partial
100911693	−11.58699	Down	1.35E-199	LOC100911693	Eukaryotic translation initiation factor 4 gamma 1-like

Abbreviations: EXPT: SRF group; CTRL: Con group.

differences were observed in the tested apoptosis proteins among different groups. For the rats exposed to SRF-EMR for 100 days, only cleaved-caspase8 was significantly upregulated in the SRF group when compared with the Con group. For the rats exposed to SRF-EMR for 150 days, only the level of Bcl-2 was lower, while the levels of Bax, cleaved-caspase-3, Fas, FasL and cleaved-caspase-8 were significantly higher in the SRF group versus the Con group. Thus, long-term exposure to SRF-EMR upregulated the apoptosis level in the testes of rats.

3.4. SRF-EMR exposure upregulates testicular Spock3

To characterize the transcriptional profile changes in the rats exposed to SRF-EMR, we compared the gene profiles from mRNA-seq data of the Con group (named CTRL group in Fig. 5) to the SRF group (named EXPT group in Fig. 5). As shown in Fig. 5A, a total of 1663 differentially expressed genes including 1446 up-regulated and 217 down-regulated genes were identified. To validate the accuracy of mRNA-seq analysis, 22 selected genes were analyzed by RT-qPCR. 77.27% selected genes in RT-qPCR showed concordant change patterns with mRNA-seq, and there was a positive correlation ($R = 0.843$ for Pearson correlation analysis, $P < 0.001$) between mRNA-Seq and RT-qPCR results (Fig. 5B), confirming its reliability. Thirteen differentially expressed genes with a log2 Ratio(EXPT/CTRL) higher than 8 and a q-value <0.01 were further screened out for analysis (Table 2). Among these genes, Spock3, a member of the BM-40/SPARC/Osteonectin family of modular extracellular proteins (Charbonnier et al., 1998), drew our attention because of its role in modulating the cell-cell junction via metalloendopeptidase inhibitor activity (Hartmann et al., 2013; Nakada et al., 2001), while the blood–testis barrier (BTB) is an important cell–cell junction that is key to the normal spermatogenesis in rats (Mruk and Cheng, 2015). Interestingly, the Spock3 level was higher in rats exposed to SRF-EMR for 150 days compared with the unexposed Con group. Meanwhile, no significant difference was observed between the Con and Nor groups (Fig. 5C–D).

3.5. Inhibiting Spock3 overexpression alleviated testicular injury and restored sperm quality in SRF-EMR exposed rats

Lentivirus transfection was performed and Spock3 knockdown was successfully achieved in the testes of rats (Fig. S2). After 150 days of exposure, sperm quality was improved in the SRF + LV-SP3 group when compared with the SRF group whereas no significant difference was observed between the SRF and SRF + LV-NC groups (Fig. 6A). The morphological analysis also showed the improvement of the epithelium height and the Johnsen score in the SRF + LV-SP3 group as compared with the SRF group. Meanwhile, no significant difference was found between the SRF and SRF + LV-NC groups (Fig. 6B–C).

Furthermore, oxidative stress products were lower and anti-oxidative enzymes were higher in the SRF + LV-SP3 group compared to the SRF group (Fig. 6D). A decrease in the apoptotic proteins was also observed in the SRF + LV-SP3 group (Fig. 6E–F). Thus, inhibiting Spock3 overexpression ameliorated the SRF-EMR induced testicular injury and restored sperm quality in rats exposed to long-term SRF-EMR.

3.6. Inhibiting Spock3 overexpression rescued BTB disorder in rats exposed to SRF-EMR for 150 days

BTB was evaluated in rats exposed to SRF-EMR for 150 days. As shown in Fig. 7A–B, compared with the Con group, the apical ectoplasmic-specialization (ES) proteins including laminin-γ3 and nectin-3 as well as the adherens junction (AJ) protein β1-integrin, were higher in the SRF group. Conversely, the basal tight-junction (TJ) proteins including occludin, zonula occludens-1 (ZO-1) and coxsackie and adenovirus receptor (CAR) as well as the basal ES protein N-Cadherin, were lower in the SRF group than in the Con group. These results revealed that BTB was damaged in rats after long-term exposure to SRF-EMR. As compared with the SRF group, in the SRF + LV-SP3 group, the levels of apical ES proteins and AJ protein were lower, while those of TJ proteins were higher. The immunofluorescence staining analysis showed that laminin-γ3 and nectin-3 were primarily upregulated on the luminal surface while occludin was primarily downregulated on the basal surface in the SRF group (Fig. 7C). Together, these results indicated that long-term exposure to SRF-EMR disturbed BTB by upregulating Spock3.

3.7. Long-term SRF-EMR exposure promoted the formation of MMP14-Spock3 complex by increasing Spock3 in rats

Results from the co-immunoprecipitation experiment showed that the ratio of Spock3 to the precursor of matrix metalloproteinase 2 (P-MMP2)—both of which bind to matrix metalloproteinase 14 (MMP14)—was relatively higher in the SRF group than in the Con group. Further analysis showed that this ratio was downregulated in the SRF + LV-SP3 group when compared with the SRF group (Fig. 8A–B). These results revealed that long-term SRF-EMR exposure increased the protein level of Spock3 binding to MMP14 but relatively decreased the level of P-MMP2 binding to MMP14, suggesting that SRF-EMR promoted the formation of the MMP14–Spock3 complex and decreased the formation of the MMP14–P-MMP2 complex.

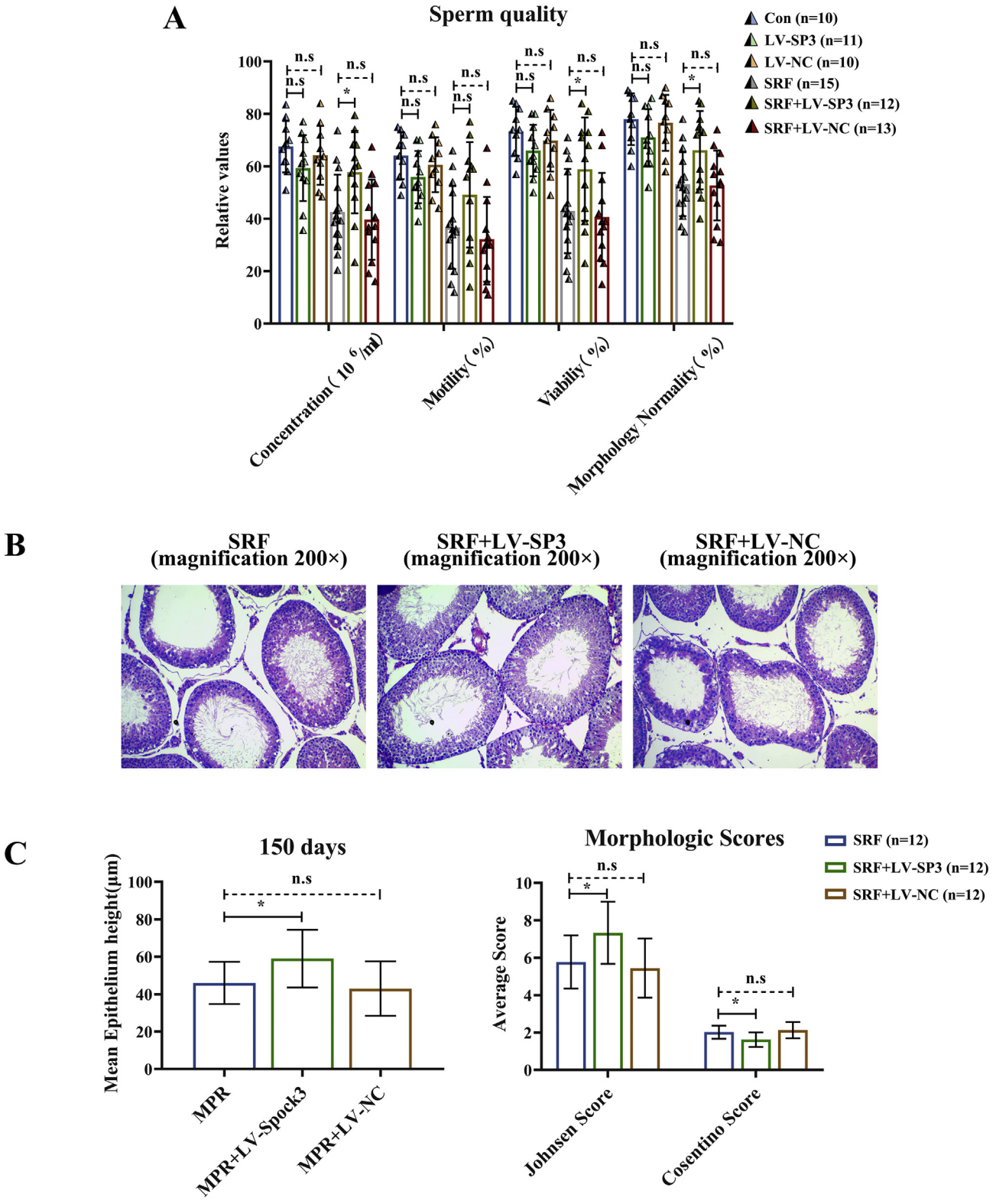


Fig. 6. Inhibiting Spock-3 overexpression alleviated testicular injury and restored sperm quality in rats. LV-Spock3 lentivirus was applied to inhibit testicular Spock3 via intratesticular injection in rats exposed to SRF-EMR for 100 days. Then sperm quality and testicular injury were evaluated after 150 days of SRF-EMR exposure. (A) Values of sperm quality. LV-Spock3 lentivirus significantly improved sperm quality, except sperm motility in rats. (B–C) Representative images and morphologic scores of H&E staining in rat testes (original magnification 200×). LV-Spock3 lentivirus increased the epithelium height and Johnsen score in rats exposed to SRF-EMR for 150 days. (D) Relative values of the oxidative–antioxidative system in the testes of rats. LV-Spock3 lentivirus significantly upregulated SOD and CAT but downregulated MDA and 4-HNE in the exposed rats. (E–F) Representative western-blotting images and relative density changes of apoptosis proteins in the testes of rats. LV-Spock3 lentivirus significantly improved testicular apoptosis in the exposed rats. Each bar in histogram represents Mean ± SD. Abbreviation and symbol, P-Caspase: precursor caspase, C-Caspase: cleaved caspase, n.s: no significant difference ($P > 0.05$), *: $P < 0.05$, **: $P < 0.01$.

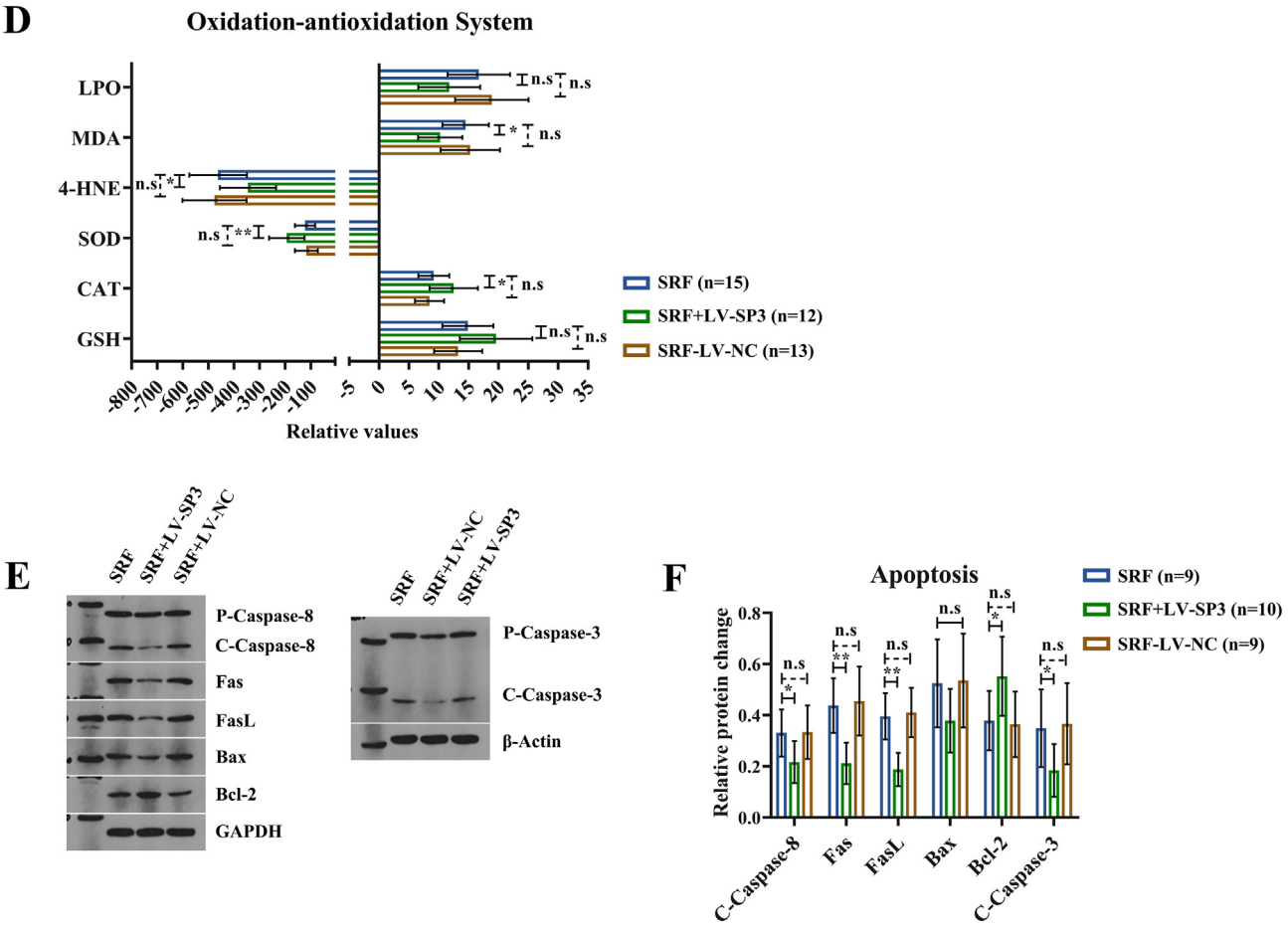


Fig. 6 (*continued*).

3.8. Regulation of the Spock3–MMP2 axis was involved in the biological effect of SRF-EMR on the testes of rats

Immunoblotting (Input) showed that the ratio of active-MMP2 to pro-MMP2 was relatively lower in the SRF group as compared with the Con group. Nevertheless, this ratio was higher in the SRF + LV-SP3 group than in the SRF group (Fig. 8A and C). These results indicated that SRF-EMR suppressed MMP2 activity via upregulating Spock3 expression.

In addition, the protein level of MMP14 was higher in the SRF group as compared with the Con group whereas the MMP14 expression was lower in the SRF + LV-SP3 group than in the SRF group (Fig. 8A and C).

4. Discussion

According to the statistics, nearly 4.77 billion people worldwide are using smartphones and are exposed to SRF-EMR (Al-Serori et al., 2017). Although the adverse effect of SRF-EMR on male fertility has gradually become the concern of modern society, it has not been thoroughly investigated. To date, the studies on humans and animals that have investigated the effect of SRF-EMR have shown equivocal and controversial results. Furthermore, most of these studies have focused on the reproductive effects of SRF-EMR exposure on the whole body or head while few have investigated the direct effect of SRF-EMR on the testes (Adams et al., 2014; Houston et al., 2016; Liu et al., 2014). The present study explored this topic in adult rats by using a special SRF-EMR exposure model in which the reproductive effects of hyperthermia and mental stress were minimized as much as possible (As Fig. 1 showed). To our knowledge, for the first time, our results demonstrated that long-term exposure to 4G SRF-EMR directly impaired the testes and male reproductive potential in rats. Although some previous studies considered that short-term whole-body exposure to SRF-EMR at standard energy doses did not suppress sperm quality (Dasdag et al., 2003; Tumkaya et al., 2016), Ribeiro and Sepehrimanesh, after further analysis, found that such short-term exposure led to ultrastructural or non-thermal stress related proteomic changes in the testes (Ribeiro et al., 2007; Sepehrimanesh et al., 2014; Sepehrimanesh et al., 2017). Similarly, Yan conducted long-term whole-body exposure to SRF-EMR by using a smartphone and found that SRF-EMR increased incidence of sperm death and aberration rate of sperm in rats (Yan et al., 2007), while Shahin demonstrated that long-term systemic exposure to SRF-EMR led to oxidative stress injury and apoptosis in the testes of mice (Shahin et al., 2018). The results of these previous studies, along with our results strongly support that long-term SRF-EMR exposure could adversely affect male fertility in rats, which might be attributed to certain accumulative biological effects of SRF-EMR on the testes.

In the mating experiment, SRF-EMR led to pup weight loss of male rats exposed to SRF-EMR for 150 days, which might be attributed to the high rate of sperm deformation. This result was consistent with the finding of Kesari (Kesari and Behari, 2012) who showed that pup weight and litter size of SRF-EMR-exposed male rats decreased after systemic exposure to SRF-EMR for 45 days. Nevertheless, in this study, the mating experiment did not indicate other statistically significant changes in these rats, despite their impaired sperm quality. This

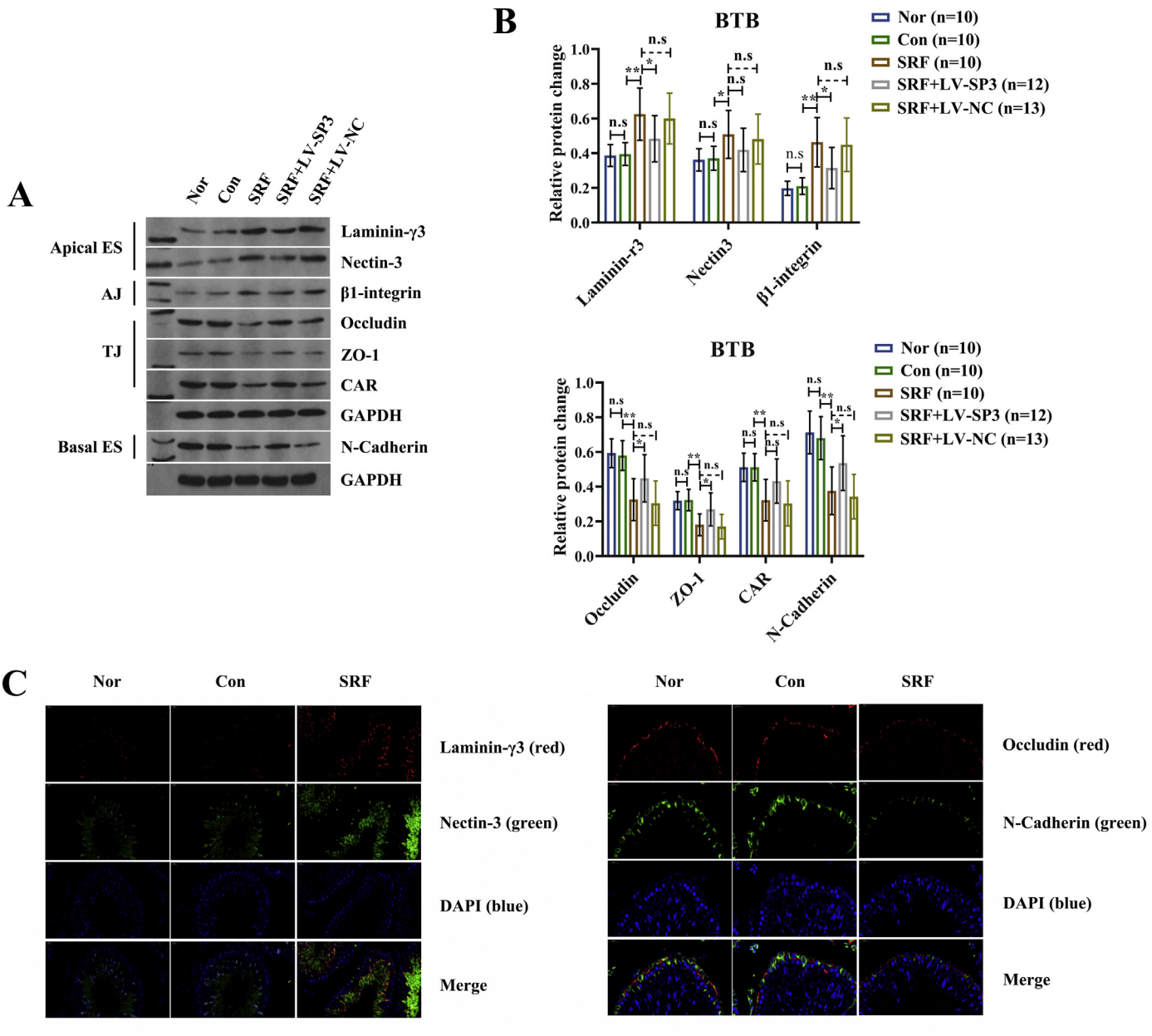


Fig. 7. Inhibiting Spock3 overexpression rescued BTB disorder in rats exposed to SRF-EMR for 150 days. BTB was evaluated via western blotting and immunofluorescence in rats exposed to SRF-EMR for 150 days. (A–B) Representative western-blotting images and relative density changes of BTB proteins in rats exposed to SRF-EMR for 150 days. SRF-EMR significantly increased apical ES protein expression, including laminin-γ3 and nectin-3, as well as AJ protein β1-integrin. Meanwhile, it decreased TJ protein expressions including occludin, ZO-1, and CAR, as well as basal ES protein N-Cadherin in rats. However, LV-Spock3 lentivirus downregulated laminin-γ3 and β1-integrin while upregulating occludin, ZO-1, CAR, and N-Cadherin in the exposed rats. (C) Representative immunofluorescence images of rats ($n = 7$–9). In the seminiferous tubules, the laminin-γ3 was co-localized with nectin-3 on the luminal surface, and their fluorescence intensities were comparatively higher in the SRF group than in the Con group. The occludin was co-localized with N-Cadherin on the basal side, and their fluorescence intensities were comparatively lower in the SRF group than in the Con group. Each bar in histogram represents Mean ± SD. Abbreviation and symbol, n.s: no significant difference ($P > 0.05$), *: $P < 0.05$, **: $P < 0.01$.

seemingly contradictory result might be attributed to the strong reproductive compensatory potential of male SD rats and the limitations of the currently-used evaluation indexes in our mating experiment. Thus, future studies should pay attention to other changes, especially genetic abnormalities, in the offspring of rats exposed to SRF-EMR for a long time, and further clarify the involved mechanisms leading to the abnormalities in their offspring.

Based on the sequencing results, we further investigated the relationship between Spock3 overexpression and sperm quality decline as well as BTB disorder in rats exposed to SRF-EMR for 150 days, which has not been discussed before. The results showed that inhibiting Spock3 overexpression alleviated sperm quality decline and reversed BTB damage in these rats. Since ameliorating BTB disorder could improve testicular injury and sperm quality (Cheng, 2014), it was rational to conclude that long-term exposure to SRF-EMR suppressed sperm quality via Spock3-mediated BTB disorder in rats. Thus, besides the blood-brain barrier (Kim et al., 2017; Nittby et al., 2009), BTB is another biological target of SRF-EMR.

Our results showed that SRF-EMR promoted the formation of MMP14–Spock3 complex, suppressed the formation of MMP14–P-MMP2 complex, and inhibited MMP2 activity in rats after long-term exposure, which were mediated via Spock3 overexpression in the testes of

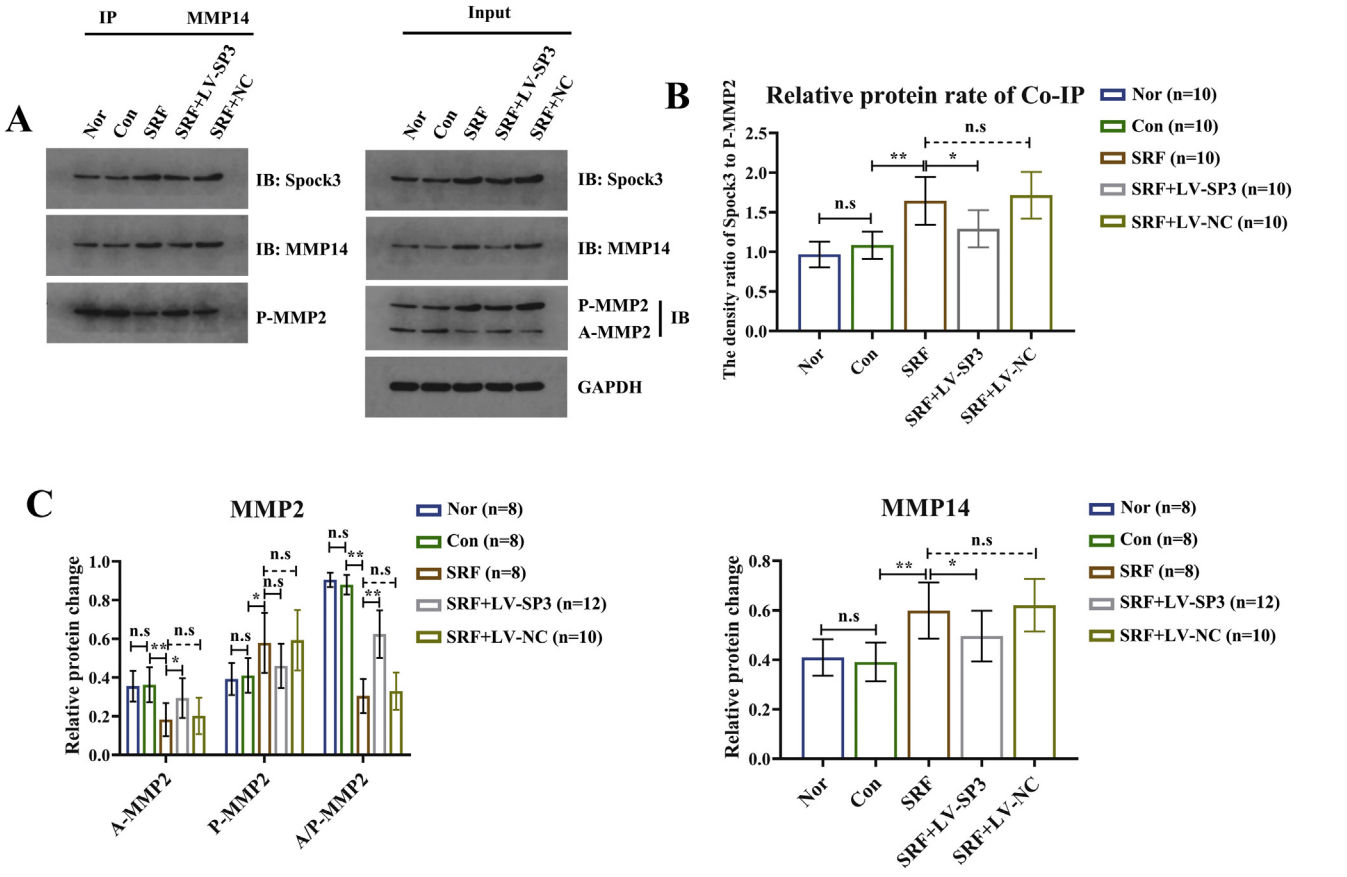


Fig. 8. Spock3–MMP axis regulation was involved in the biological effect of SRF-EMR on the testes of rats. MMPs were detected via co-immunoprecipitation and western blotting in the testes of rats exposed to SRF-EMR for 150 days. (A–B) Representative co-immunoprecipitation images and density ratios of Spock3 to P-MMP2 in rats The density ratio of Spock3 to P-MMP2 was higher in the SRF group as compared with the Con group, whereas LV-Spock3 lentivirus reversed this change. (C) Relative immunoblotting density changes (Input) of MMPs in rats. SRF-EMR significantly decreased active MMP2 level and increased MMP14 level in rats while LV-Spock3 lentivirus significantly reversed these changes. Each bar in histogram represents Mean ± SD. Abbreviation and symbol, A-MMP2: active MMP2, P-MMP2: precursor MMP2, IB: immunoblotting, n.s: no significant difference ($P > 0.05$), *: $P < 0.05$, **: $P < 0.01$.

rats. Previous studies have shown that Spock3 disrupted the formation of MMP14-P-MMP2 by forming a complex with MMP14, thereby inhibiting MMP2 activation (Hartmann et al., 2013; Nakada et al., 2001; Sounni et al., 2003). Thus, SRF-EMR might inhibit MMP2 activity via the Spock3-MMPs axis in the testes of rats exposed to SRF-EMR. In the BTB cycle, activated MMP2 promotes circulation by acting on laminin-γ3 to dissociate the apical ES complex and promoted continuous migration of germ cells in the seminiferous tubules (Cheng and Mruk, 2010; Longin et al., 2001; Siu and Cheng, 2004; Yan et al., 2008b). Therefore, suppressing MMP2 activity could block the BTB cycle and impair spermatogenesis (Chen et al., 2011).

These results support the fact that suppressing MMP2 activity might be a participating mechanism involved in Spock3-mediated BTB disorder in rats exposed to SRF-EMR. However, our results could not distinguish whether inhibiting MMP2 activity was the primary downstream mechanism in Spock3-mediated BTB disorder, which is still being investigated in our lab.

Although the amount of P-MMP2 binding to MMP14 decreased, the total amount of MMP14 increased in rats exposed to SRF-EMR for 150 days. These results might be due to the compensatory mechanism aimed to stabilize MMP homeostasis by upregulating the total amount of MMP14 under this abnormal condition. Perhaps by prolonging the modeling time, this compensatory mechanism would be further disturbed.

Our results provide us with a hypothesis regarding the mechanism (Fig. 9) by which long-term exposure to SRF-EMR suppresses male reproductive potential in adult rats. The mechanism may work by gradually inhibiting the disassembly of the apical ES complex by regulating Spock3–MMP2 axis in the testes of rats, leading to the accumulation of intact apical ES components and the reduction of activated apical ES fragments needed for the BTB recycling. Since the activated apical ES fragments could induce the disassembly of other BTB components such as TJ (which is crucial to facilitate germ cell migration), spermatogenesis is disrupted and secondary germ cell apoptosis gradually increases, accompanied by the degradation of redundant BTB components. Furthermore, a sufficient amount of activated apical ES fragments is needed to ensure that a sufficient number of fibrils from "old" BTB components participate in the recycling (Cheng and Mruk, 2009; Cheng and Mruk, 2010). Thus, the amount of "new" BTB components decreases with the reduction of "old" BTB fibrils. As a result, a vicious cycle forms even though a portion of the decreasing fibrils might be temporarily supplemented to alleviate BTB disorder by inhibiting degradation in continuous transcytosis or accelerating biosynthesis in BTB recycle (Stamatovic et al., 2017; Yan et al., 2008a). These events may finally impair BTB and male fertility in rats.

A national toxicology program in America has raised concerns about the adverse effects of SRF-EMR on certain specific organs since they recently found that long-term systemic 2G or 3G SRF-EMR exposure increased the risks of malignant brain gliomas and heart schwannomas in rats (NIEHS, 2018). Although the exposure intensity of the SRF-EMR used in our study was much stronger than that in reality owing to the short exposure distance and the continuous exposure pattern, it is nevertheless rational to conclude that long-term exposure to 4G SRF-EMR could suppress male reproductive potential by directly impairing the

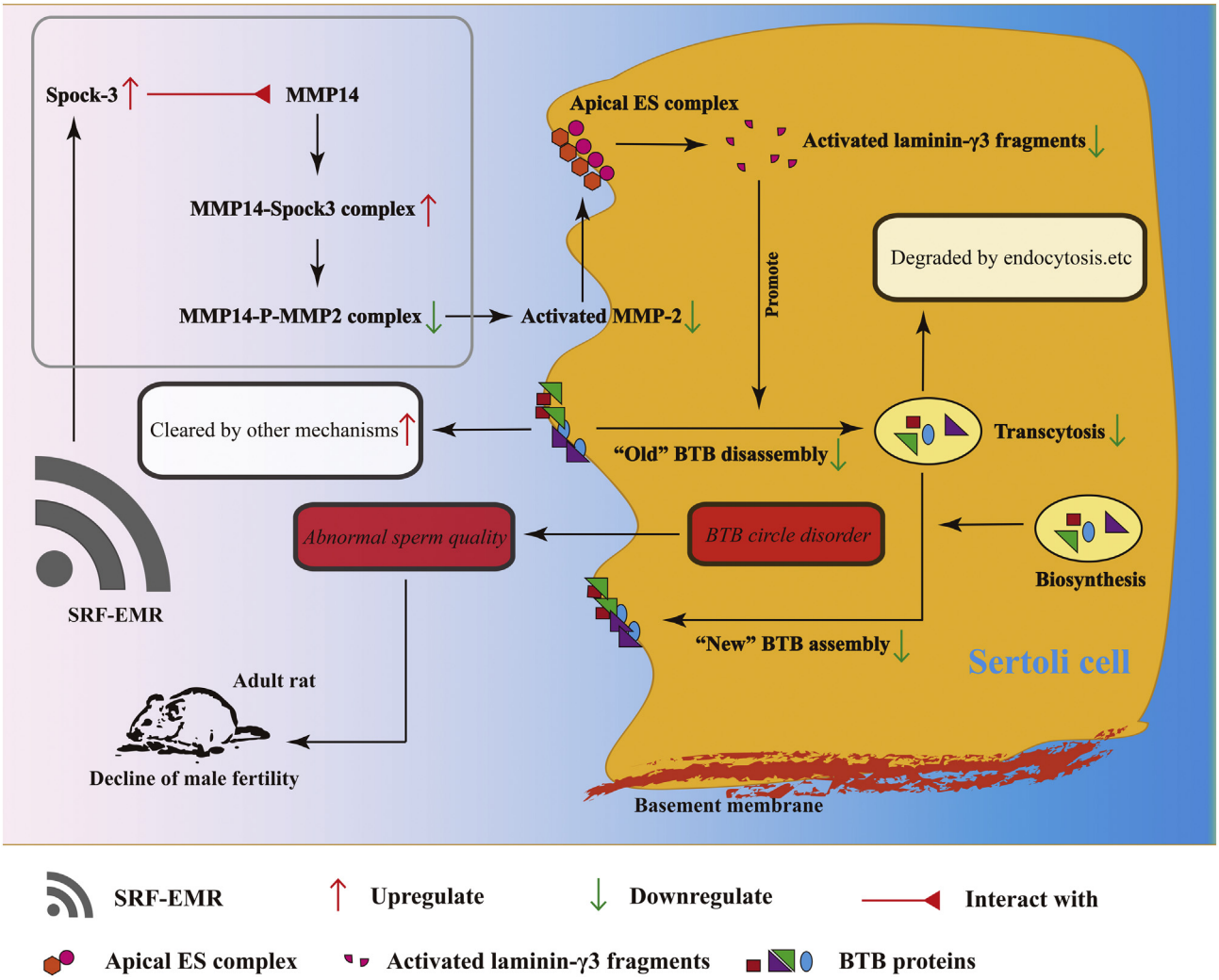


Fig. 9. Possible mechanism by which long-term SRF-EMR exposure decreased the fertility potential of male adult rats. After long-term local exposure, SRF-EMR gradually inhibited the disassembly of the apical ES complex by regulating the Spock3–MMP2 axis in the testes of rats, resulting in the decrease of activated apical laminin-γ3 fragments in the BTB recycling. Since the activated laminin-γ3 fragments could induce the disassembly of other BTB components to facilitate germ cell migration, spermatogenesis was disrupted and secondary apoptosis of germ cells gradually increased, accompanied by the degradation of redundant BTB components. Additionally, the "new" BTB components would also decrease along with the reduction of disassembled "old" BTB fibrils. As a result, normal BTB recycling would be gradually impaired even though a portion of decreasing BTB fibrils might be temporarily supplemented to alleviate BTB disorder by inhibiting degradation in continuous transcytosis or accelerating biosynthesis in recycling. Finally, these events would decrease sperm quality and suppress male fertility in rats.

testes. Thus, before this issue is fully elaborated, men are advised to keep smartphones away from their testes to avoid potential adverse effects of this neglected low-energy radiation. Given the limitations of this study, additional studies on SRF-EMR with increased exposure duration and different working models of smartphones should be conducted to further confirm the current conclusion along with investigating additional reproductive effects of SRF-EMR. Furthermore, SRF-EMR belongs to RF-EMR, which is emitted by other sources common in daily life such as phone towers and electric substations. Now that the adverse effects of long-term SRF-EMR exposure have been presented, future studies should pay more attention to the long-term health effects of other RF-EMRs with higher energy. These health effects may prove more important in the upcoming 5G era, when more RF-EMRs would be brought into our daily life.

5. Conclusion

Long-term exposure to 4G SRF-EMR diminished the reproductive potential of adult male rats by directly disrupting the Spock3–BTB axis in the testes, in which inhibiting MMP2 activity might be an important mechanism involved. This study, thus, contributed to revealing the ambiguous relationship between male subfertility and smartphone use.

Acknowledgements

This work is supported by the Finance Science and Technology Project of Hainan Province under Grant [number ZDXM2013006], the Finance Science and Technology Project of Hainan Province under Grant [number ZDYF2017084] and the Hainan Provincial Natural Science Foundation of China under Grant [number 818MS134]. We thank Foundview Laboratory (Beijing, China) for their technical assistance.

Declaration of competing interest

None.

Appendix A. Supplementary data

Supplementary data to this article can be found online at https://doi.org/10.1016/j.scitotenv.2019.133860.

References

Adams, J.A., Galloway, T.S., Mondal, D., Esteves, S.C., Mathews, F., 2014. Effect of mobile telephones on sperm quality: a systematic review and meta-analysis. Environ. Int. 70, 106–112.

Agarwal, A., Singh, A., Hamada, A., Kesari, K., 2011. Cell phones and male infertility: a review of recent innovations in technology and consequences. Int. Braz. J. Urol. 37, 432–454.

Al-Serori, H., Kundi, M., Ferk, F., Misik, M., Nersesyan, A., Murbach, M., et al., 2017. Evaluation of the potential of mobile phone specific electromagnetic fields (UMTS) to produce micronuclei in human glioblastoma cell lines. Toxicol. in Vitro 40, 264–271.

Belpomme, D., Hardell, L., Belyaev, I., Burgio, E., Carpenter, D.O., 2018. Thermal and non-thermal health effects of low intensity non-ionizing radiation: an international perspective. Environ. Pollut. 242, 643–658.

Bielsa-Fernandez, P., Rodriguez-Martin, B., 2018. Association between radiation from mobile phones and tumour risk in adults. Gac. Sanit. 32, 81–91.

Bolte, J.F., Eikelboom, T., 2012. Personal radiofrequency electromagnetic field measurements in the Netherlands: exposure level and variability for everyday activities, times of day and types of area. Environ. Int. 48, 133–142.

Charbonnier, F., Perin, J.P., Mattei, M.G., Camuzat, A., Bonnet, F., Gressin, L., et al., 1998. Genomic organization of the human SPOCK gene and its chromosomal localization to 5q31. Genomics 48, 377–380.

Chen, H., Fok, K.L., Yu, S., Jiang, J., Chen, Z., Gui, Y., et al., 2011. CD147 is required for matrix metalloproteinases-2 production and germ cell migration during spermatogenesis. Mol. Hum. Reprod. 17, 405–414.

Cheng, C.Y., 2014. Toxicants target cell junctions in the testis: insights from the indazole-carboxylic acid model. Spermatogenesis 4, e981485.

Cheng, C.Y., Mruk, D.D., 2009. An intracellular trafficking pathway in the seminiferous epithelium regulating spermatogenesis: a biochemical and molecular perspective. Crit. Rev. Biochem. Mol. Biol. 44, 245–263.

Cheng, C.Y., Mruk, D.D., 2010. A local autocrine axis in the testes that regulates spermatogenesis. Nat Rev Endocrinol 6, 380–395.

Dasdag, S., Zulkuf Akdag, M., Aksen, F., Yilmaz, F., Bashan, M., Mutlu Dasdag, M., et al., 2003. Whole body exposure of rats to microwaves emitted from a cell phone does not affect the testes. Bioelectromagnetics 24, 182–188.

Eeftens, M., Struchen, B., Birks, L.E., Cardis, E., Estarlich, M., Fernandez, M.F., et al., 2018. Personal exposure to radio-frequency electromagnetic fields in Europe: is there a generation gap? Environ. Int. 121, 216–226.

Falcioni, L., Bua, L., Tibaldi, E., Lauriola, M., De Angelis, L., Gnudi, F., et al., 2018. Report of final results regarding brain and heart tumors in Sprague-Dawley rats exposed from prenatal life until natural death to mobile phone radiofrequency field representative of a 1.8GHz GSM base station environmental emission. Environ. Res. 165, 496–503.

Hartmann, U., Hulsmann, H., Seul, J., Roll, S., Midani, H., Breloy, I., et al., 2013. Testican-3: a brain-specific proteoglycan member of the BM-40/SPARC/osteonectin family. J. Neurochem. 125, 399–409.

Houston, B.J., Nixon, B., King, B.V., De Iuliis, G.N., Aitken, R.J., 2016. The effects of radiofrequency electromagnetic radiation on sperm function. Reproduction 152, R263–r276.

IARC, 2013. Non-ionizing Radiation, Part 2: Radiofrequency Electromagnetic Fields. vol 102.

Kesari, K.K., Behari, J., 2012. Evidence for mobile phone radiation exposure effects on reproductive pattern of male rats: role of ROS. Electromagn Biol Med 31, 213–222.

Kesari, K.K., Agarwal, A., Henkel, R., 2018. Radiations and male fertility. Reprod. Biol. Endocrinol. 16, 118.

Kim, J.H., Yu, D.H., Huh, Y.H., Lee, E.H., Kim, H.G., Kim, H.R., 2017. Long-term exposure to 835 MHz RF-EMF induces hyperactivity, autophagy and demyelination in the cortical neurons of mice. Sci. Rep. 7, 41129.

Kwon, M.S., Hamalainen, H., 2011. Effects of mobile phone electromagnetic fields: critical evaluation of behavioral and neurophysiological studies. Bioelectromagnetics 32, 253–272.

Liu, K., Li, Y., Zhang, G., Liu, J., Cao, J., Ao, L., et al., 2014. Association between mobile phone use and semen quality: a systemic review and meta-analysis. Andrology 2, 491–501.

Longin, J., Guillaumot, P., Chauvin, M.A., Morera, A.M., Le Magueresse-Battistoni, B., 2001. MT1-MMP in rat testicular development and the control of Sertoli cell proMMP-2 activation. J. Cell Sci. 114, 2125–2134.

Mruk, D.D., Cheng, C.Y., 2015. The mammalian blood-testis barrier: its biology and regulation. Endocr. Rev. 36, 564–591.

Nakada, M., Yamada, A., Takino, T., Miyamori, H., Takahashi, T., Yamashita, J., et al., 2001. Suppression of membrane-type 1 matrix metalloproteinase (MMP)-mediated MMP-2 activation and tumor invasion by testican 3 and its splicing variant gene product, N-Tes. Cancer Res. 61, 8896–8902.

NIEHS, 2018. Cell Phone Radio Frequency Radiation Studies. https://ntp.niehs.nih.gov/results/areas/cellphones/.

Nittby, H., Brun, A., Eberhardt, J., Malmgren, L., Persson, B.R., Salford, L.G., 2009. Increased blood-brain barrier permeability in mammalian brain 7 days after exposure to the radiation from a GSM-900 mobile phone. Pathophysiology 16, 103–112.

Repacholi, M.H., Lerchl, A., Roosli, M., Sienkiewicz, Z., Auvinen, A., Breckenkamp, J., et al., 2012. Systematic review of wireless phone use and brain cancer and other head tumors. Bioelectromagnetics 33, 187–206.

Ribeiro, E.P., Rhoden, E.L., Horn, M.M., Rhoden, C., Lima, L.P., Toniolo, L., 2007. Effects of subchronic exposure to radio frequency from a conventional cellular telephone on testicular function in adult rats. J. Urol. 177, 395–399.

Santini, S.J., Cordone, V., Falone, S., Mijit, M., Tatone, C., Amicarelli, F., et al., 2018. Role of mitochondria in the oxidative stress induced by electromagnetic fields: focus on reproductive systems. Oxidative Med. Cell. Longev. 2018, 5076271.

Sepehrimanesh, M., Davis, D.L., 2016. Proteomic impacts of electromagnetic fields on the male reproductive system. Comp. Clin. Pathol. 26, 309–313.

Sepehrimanesh, M., Kazemipour, N., Saeb, M., Nazifi, S., 2014. Analysis of rat testicular proteome following 30-day exposure to 900 MHz electromagnetic field radiation. Electrophoresis 35, 3331–3338.

Sepehrimanesh, M., Kazemipour, N., Saeb, M., Nazifi, S., Davis, D.L., 2017. Proteomic analysis of continuous 900-MHz radiofrequency electromagnetic field exposure in testicular tissue: a rat model of human cell phone exposure. Environ. Sci. Pollut. Res. Int. 24, 13666–13673.

Shahin, S., Singh, S.P., Chaturvedi, C.M., 2018. 1800 MHz mobile phone irradiation induced oxidative and nitrosative stress leads to p53 dependent Bax mediated testicular apoptosis in mice, Mus musculus. J. Cell. Physiol. 233, 7253–7267.

Siu, M.K., Cheng, C.Y., 2004. Interactions of proteases, protease inhibitors, and the beta1 integrin/laminin gamma3 protein complex in the regulation of ectoplasmic specialization dynamics in the rat testis. Biol. Reprod. 70, 945–964.

Sounni, N.E., Janssen, M., Foidart, J.M., Noel, A., 2003. Membrane type-1 matrix metalloproteinase and TIMP-2 in tumor angiogenesis. Matrix Biol. 22, 55–61.

Stamatovic, S.M., Johnson, A.M., Sladojevic, N., Keep, R.F., Andjelkovic, A.V., 2017. Endocytosis of tight junction proteins and the regulation of degradation and recycling. Ann. N. Y. Acad. Sci. 1397, 54–65.

Tumkaya, L., Kalkan, Y., Bas, O., Yilmaz, A., 2016. Mobile phone radiation during pubertal development has no effect on testicular histology in rats. Toxicol. Ind. Health 32, 328–336.

Vahedi, Z., Saiphoo, A., 2018. The association between smartphone use, stress, and anxiety: a meta-analytic review. Stress. Health 34, 347–358.

Viel, J.F., Cardis, E., Moissonnier, M., de Seze, R., Hours, M., 2009. Radiofrequency exposure in the French general population: band, time, location and activity variability. Environ. Int. 35, 1150–1154.

Wang, L., Feng, Z., Wang, X., Wang, X., Zhang, X., 2010. DEGseq: an R package for identifying differentially expressed genes from RNA-seq data. Bioinformatics 26, 136–138.

Wu, Y., Chen, X., Wang, S., Jiang, M., Zheng, B., Zhou, Q., et al., 2012. Flotillin-2 is an acrosome-related protein involved in mouse spermiogenesis. J. Biomed. Res. 26, 278–287.

Yan, J.G., Agresti, M., Bruce, T., Yan, Y.H., Granlund, A., Matloub, H.S., 2007. Effects of cellular phone emissions on sperm motility in rats. Fertil. Steril. 88, 957–964.

Yan, H.H., Mruk, D.D., Lee, W.M., Cheng, C.Y., 2008a. Blood-testis barrier dynamics are regulated by testosterone and cytokines via their differential effects on the kinetics of protein endocytosis and recycling in Sertoli cells. FASEB J. 22, 1945–1959.

Yan, H.H., Mruk, D.D., Wong, E.W., Lee, W.M., Cheng, C.Y., 2008b. An autocrine axis in the testis that coordinates spermiation and blood-testis barrier restructuring during spermatogenesis. Proc. Natl. Acad. Sci. U. S. A. 105, 8950–8955.

Zohni, K., Zhang, X., Tan, S.L., Chan, P., Nagano, M.C., 2012. The efficiency of male fertility restoration is dependent on the recovery kinetics of spermatogonial stem cells after cytotoxic treatment with busulfan in mice. Hum. Reprod. 27, 44–53.